Optics & Laser Technology 77 (2016) 40–50

Contents lists available at ScienceDirect

Optics & Laser Technology

journal homepage: www.elsevier.com/locate/optlastec

Investigation of the inhomogeneity of atmospheric turbulence at day and night times

Saifollah Rasouli [a,b,*], Y. Rajabi [a]

[a] Department of Physics, Institute for Advanced Studies in Basic Sciences (IASBS), Zanjan 45137-66731, Iran
[b] Optics Research Center, Institute for Advanced Studies in Basic Sciences (IASBS), Zanjan 45137-66731, Iran

ARTICLE INFO

Article history:
Received 6 July 2015
Received in revised form
16 August 2015
Accepted 23 August 2015

Keywords:
Atmospheric turbulence
Moiré techniques
Telescopes
Talbot and self-imaging effects

ABSTRACT

In this work, we introduce for the first time the use of a pair of telescopes facing each other in conjunction with the use of a pair of moiré deflectometers for the investigation of the inhomogeneity of atmospheric turbulence. In the experiment, a laser beam enters a telescope from its back focal point by virtue of a focusing lens and is expanded and re-collimated by it before passing through the turbulent ground level atmosphere. It then enters the aperture of a second telescope, where it is again re-collimated behind the focal point, finally entering a pair of moiré deflectometers. We use the instrument for measuring the fluctuations of two components of the angle of arrival (AA) across the second telescope's aperture. Calculation of the structure functions of the vertical and horizontal components of the AA fluctuations on the second telescope's aperture (over typical vertical and horizontal moiré fringes) at different altitudes and at different latitudes allows a quantitative measure of the inhomogeneity at the day and night times in the atmospheric surface layer. Experimental results show that on sunny days the difference between the structure functions of the horizontal component of the AA fluctuations calculated at two different altitudes over two horizontal moiré fringes is changed as a function of the time and its value meaningfully correlated to the mean value of the temperature of the Earth's surface. We did not find any interpretative correlation for the difference between the structure functions of the vertical component of the AA fluctuations calculated at two different latitudes. In addition, for the data recorded on windy days the observed correlation between the inhomogeneity of the atmospheric turbulence and the Earth's temperature almost disappeared.

1. Introduction

In recent years, a considerable number of theoretical and experimental studies have challenged the isotropy and homogeneity of atmospheric turbulence. Theoretical studies predict and experimental results show that the statistics of a light beam propagating through the atmosphere does not always guarantee the homogeneity and isotropy of the atmospheric turbulence [1–4]. In addition, significant inhomogeneity and anisotropy in indoor convective air turbulence in the presence of a 2D temperature gradient are reported [5]. Determining and introducing the sources of the observed inhomogeneity and anisotropy of atmospheric turbulence is an important issue and results can help us to look into new concepts in establishing a comprehensive theory for atmospheric turbulence. In this connection, it seems that precise attention to the boundary conditions of atmospheric turbulence and their changes during the day and night times are very important. The Earth's surface is the atmosphere's primary heat source. The value of the solar energy absorbed by the Earth's surface changes during the day time. Also, the absorbed energy at day time is emitted to the atmosphere with a non-constant rate during the night time. Thus, it is reasonable to have changes in the vertical temperature gradient near the Earth's surface as a function of day and night times. On the other hand, it is worth mentioning that as different parts of the Earth's surface absorb different values of the solar energy, it is reasonable to have changes in the temperature with distance in the horizontal direction near the Earth's surface, too. This kind of temperature change is usually observed in very large areas. Therefore, it is expected that near surfaces where the texture of land is the same, the daily changes (both at the day and night times) of the vertical temperature gradient affect the observed inhomogeneity and anisotropy of the turbulence. To the best of our knowledge, until now there have been no comprehensive studies on the inhomogeneity of atmospheric

* Corresponding author at: Department of Physics, Institute for Advanced Studies in Basic Sciences (IASBS), Zanjan 45137-66731, Iran.
E-mail address: rasouli@iasbs.ac.ir (S. Rasouli).

http://dx.doi.org/10.1016/j.optlastec.2015.08.017
0030-3992/

turbulence and its behavior at the day and night times. In this work we are reporting the investigation of the effect of daily changes of the Earth's surface temperature on the homogeneity of atmospheric turbulence. It is worth mentioning that in the literature, the temperature and wind velocity changes are stated to be the main sources of the homogeneous and isotropic turbulence in which there is no dominant and stable temperature gradient such as the case occurring on the windy situations near the Earth's surface. In fact, in the atmospheric boundary layer where atmospheric dynamics are dominated by the interaction and heat exchange with the Earth's surface, there is a convective instability and it gives rise to a strong optical turbulence [6]. In the presence of wind, the existence temperature gradient near the Earth's surface is removed by the wind and as a result the turbulence passes to the homogeneous state.

Recently, we have suggested a high-sensitivity and high-resolution method for studying turbulent media based on moiré deflectometry in conjunction with a telescope [7,8]. In the mentioned references, a slightly divergent laser beam passes through turbulent ground level atmosphere and enters a telescope's aperture. These methods suffer a limitation for the investigation of inhomogeneity of the atmospheric turbulence. To study the inhomogeneity of the atmospheric turbulence, we need to compare the statistics of pairs of rays, from a light beam, separated by a constant distance over the propagation path. To this end, in this work, we use a pair of telescopes face to face in conjunction with the use of a pair of moiré deflectometers. This improvement on the set-up allows us to have a collimated and expanded laser beam with a constant beam diameter over the propagation path and as a result, the above-mentioned limitation of the pervious methods is removed.

In this paper, we report the use of a pair of telescopes standing face to face together with the use of a pair of moiré deflectometers for observing the inhomogeneity in the statistical properties of the turbulent ground level atmosphere. In addition, the behavior of the observed inhomogeneity in the day and night times is investigated. It should be mentioned that we have used the above-mentioned set-up for the investigation of the anisotropy and scaling of the phase structure function in indoor convective air turbulence in which the results will be reported elsewhere [9].

2. Experimental set-up and method of data acquisition

A schematic diagram of the experimental set-up is shown in Fig. 1. A laser beam enters a telescope by virtue of a focusing lens and is expanded and recollimated by it before passing horizontally through the turbulent ground level atmosphere and enters another telescope's aperture. The laser beam is collimated behind the second telescope's focal point by means of a collimator. The collimated beam passes through a beam splitter, and the resulting beams pass through a pair of moiré deflectometers which are installed parallel and close together.

The moiré deflectometers are installed close to each other. Directions of the gratings' rulings are almost parallel in each moiré deflectometer but are perpendicular in the two beams. Moiré patterns are formed on a plane where the second gratings of the moiré deflectometers and a diffuser are installed. The moiré patterns from both beams are projected on a CCD camera. Successive moiré patterns are recorded by the CCD camera and transferred to a computer, to allow temporal fluctuations of the AA components to be measured accurately. Displacements of the moiré fringes in the recorded patterns correspond to the fluctuations of two orthogonal components of the AA across the second telescope's aperture.

In this work we will calculate the structure function of the AA components fluctuations. For clarification of the data acquisition procedure in the calculation of the structure functions, here we present in detail the geometry of the measurements of the AA components' fluctuations from the moiré fringes displacements. In Fig. 2(a) a typical recorded frame that consists of two sets of the horizontal and vertical moiré fringes is shown. In Fig. 2(b) the corresponding low-frequency illumination distributions are shown. On the horizontal moiré fringes pattern (left side), two typical moiré fringe maxima are traced by the blue lines. Similarly, on the vertical moiré fringes pattern (right side), two typical moiré fringe maxima are traced by the red lines. For detail of the trace finding see [8,10,11]. In this report, we use the displacement data of these traces for the calculation of the structure functions of the two components of the AA fluctuations. From the displacement data of the blue traces having typical mean altitudes of y_1 and $y_2 = y_1 + \Delta y$, the structure functions of the x component of the AA fluctuations for the corresponding altitudes are to be determined. Similarly, from the displacement data of the red traces having typical mean latitudes of x_1 and $x_2 = x_1 + \Delta x$ the structure functions of the y component of the AA fluctuations at the corresponding latitudes are to be determined. All position coordinates are defined on the second telescope's aperture plane from which the real space for the position coordinates is calculated.

Due to the AA fluctuations, the moiré fringe traces are displaced. We need to calculate the mean positions of the moiré fringe traces in the determination of the AA fluctuations. In order to show the displacements of the moiré fringes, in the plots of Fig. 2(c), two pairs of the horizontal and vertical traced moiré fringes of Fig. 2(b) and their mean position traces are shown by the continuous lines and dashed lines, respectively. From the displacement of the horizontal moiré fringes in the vertical direction (the vertical separation of the adjacent continuous and dashed blue lines in Fig. 2(c)), Δy_m, the horizontal component of the AA fluctuation can be determined, α_x [10]. For given values of the blue lines' altitudes, y_1 and $y_2 = y_1 + \Delta y$, the horizontal component of the AA fluctuation α_x at all of points on the blue lines having different latitudes, x, can be determined. Similarly, from the displacement of the vertical moiré fringes in the horizontal direction

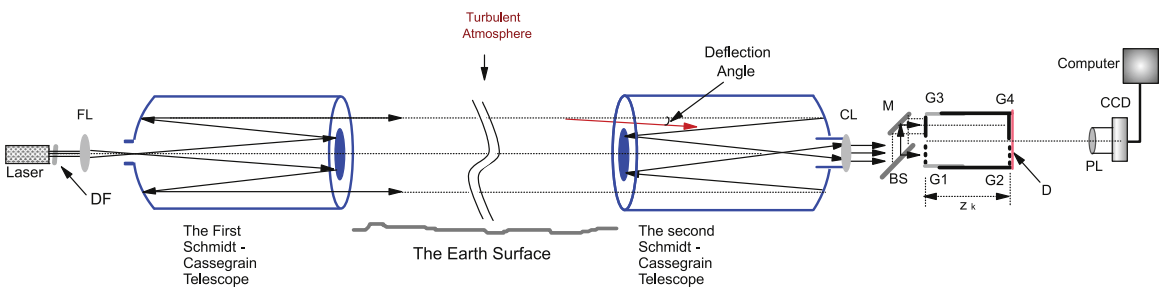

Fig. 1. Schematic diagram of the experimental set-up. *DF*, *FL*, *CL*, *BS*, *M*, D, and *PL* stand for the neutral density filter, focusing lens, collimating lens, beam splitter, mirror, diffuser, and projecting lens, respectively. G1, G2, G3 and G4 stand for the gratings.

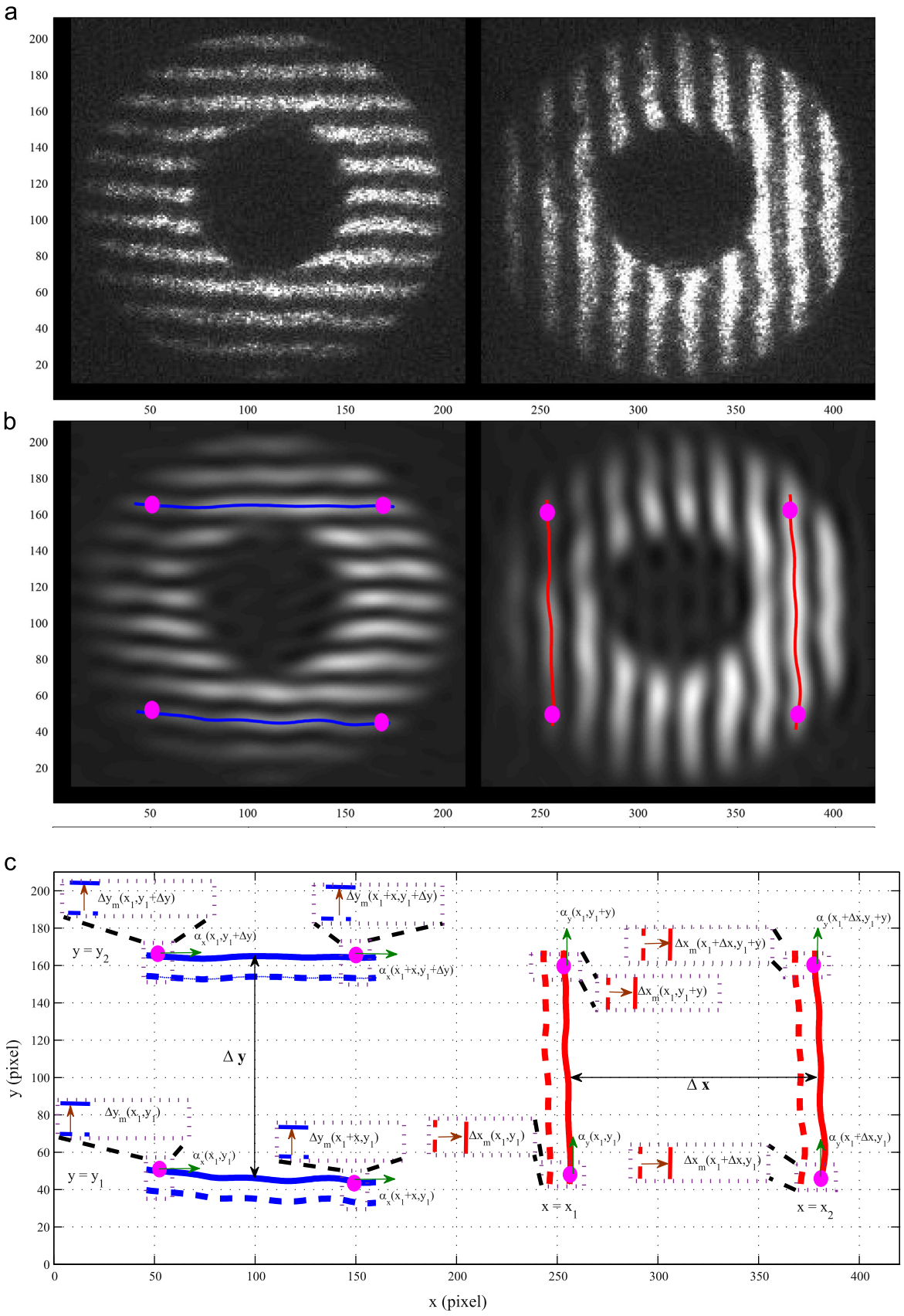

Fig. 2. (a) A typical recorded frame consists of the two sets of the orthogonal moiré patterns and (b) the corresponding low-frequency illumination distribution. The blue and red lines mark typical traces of the moiré fringe maxima in the horizontal and vertical directions, respectively. (c) Illustration of the measurements of the AA components from the displacements of the moiré fringes. The brown arrows mark typical displacements of the moiré fringes in the vertical and horizontal directions. The green arrows mark the corresponding measured AA components in the horizontal and vertical directions. The location of the four selected points are shown in (b). In each of the moiré pattern the measured AA component is parallel to the corresponding moiré fringes' traces. In the image the separation of the horizontal moiré fringes, Δy, marked by the blue color and the separation of the vertical moiré fringes, Δx, marked by the red color are equal to 14.1 cm and 13.9 cm in the real space on the second telescope's aperture plane, respectively. (For interpretation of the references to color in this figure caption, the reader is referred to the web version of this paper.)

(the horizontal separation of the adjacent continuous and dashed red lines in Fig. 2(c)), Δx_m, the vertical component of the AA fluctuation can be determined, α_y [10]. For given values of the red lines' latitudes, x_1 and $x_2 = x_1 + \Delta x$, the vertical component of the AA fluctuation α_y at all of points on the red lines having different altitudes, y, can be determined.

As stated previously, in each moiré deflectometers, the measured AA component is parallel to the corresponding moiré fringes' traces. In Fig. 2(c), the measurable components of the AA fluctuations are shown at four typical points by α_x or α_y. At the given points, the displacements of the horizontal and vertical moiré fringes' traces are illustrated by Δy_m and Δx_m, respectively. Δy and Δx show the separations of the marked moiré fringes at the horizontal and vertical fringe patterns, respectively.

Now let us present briefly the formulation of the AA fluctuations measurement from the displacements of the moiré fringes' traces. Imagine that an expanded laser beam enters the second telescope's aperture of diameter D with a local AA on that plane, α. On the image plane of the pupil, we have a laser beam of diameter $D' = \gamma D$, and the corresponding AA is equal to [7,8,12]

$$\alpha' = \frac{\alpha}{\gamma}, \tag{1}$$

where γ is the magnification of the optical system given by $\gamma = f'/f$, f is the second telescope's focal length, and f' is the focal length of the collimating lens. In the experiment, as shown in Fig. 1, the collimated beam enters a pair of moiré deflectometers. We choose a coordinate system so that in the first moiré deflectometer the grating rulings are in the x-direction and those in the second moiré deflectometer are in the y-direction. The laser beam splits into two beams by an amplitude beam splitter. The second beam is reflected by a mirror, M, in a direction parallel to the first beam's propagation direction. The beams strike the first gratings G1 and G3. The second gratings of the moiré deflectometers, G2 and G4, are separated by Z_k along its corresponding optical axis, where Z_k is the kth Talbot distance of the first gratings. The formula for the kth Talbot distance is $Z_k = 2kd^2/\lambda$, where d and λ are the grating's period and the wavelength, respectively. All gratings have equal periods d. Due to the atmospheric turbulence the self-images of the first gratings fluctuate on the second gratings. The components α'_y and α'_x of the AA fluctuation in a direction perpendicular to the lines of the gratings (parallel to the moiré trace) on the first gratings G1 and G2 are given by [11]

$$[\alpha'_x, \alpha'_y] = \frac{d}{Z_k}\left[\frac{\Delta y_m}{d'_m}, \frac{\Delta x_m}{d_m}\right], \tag{2}$$

respectively, where d_m and d'_m are the moiré fringe spacings, and Δx_m and Δy_m, as they are introduced perviously, are the moiré fringe displacements in the first and second moiré deflectometers, respectively.

Using $\alpha = \gamma\alpha'$ in Eq. (2) we obtain [7,8]

$$[\alpha_x, \alpha_y] = \frac{f'}{f}\frac{d}{Z_k}\left[\frac{\Delta y_m}{d'_m}, \frac{\Delta x_m}{d_m}\right]. \tag{3}$$

According to Eq. (3), by increasing the gratings' distance or decreasing the period of the gratings, the measurement precision can be improved.

In this work, we have used $d = 0.10$ mm, $f = 200$ cm, $f' = 13.5$ cm and $Z_k = 75$ mm. The value of Z_k of 75 mm corresponds to $k=2$. The moiré pattern in each of the moiré deflectometers consists of about 200×200 pixels and d_{m_x} and d_{m_y} were covered by 18 and 17 pixels in the corresponding moiré deflectometers, respectively. By using the sub-pixel accuracy for the displacement measurements of the traces as used in [8], the minimum measurable AA fluctuation is 5×10^{-7} rad or 0.1 arc sec.

3. Structure function of the AA fluctuations

A random function of a vector spatial variable $\mathbf{R}(x, y, z)$ and, possibly, time t is called a random field. The locally homogeneous fields of atmospheric turbulence such as the wind velocity fluctuations, temperature fluctuations, and density fluctuations are usually characterized by the structure function.

In general, the structure function for a locally homogeneous random field $u(\mathbf{R})$ can be expressed in the form

$$\begin{aligned} D_u(\mathbf{R}_1, \mathbf{R}_2) &\equiv D_u(\mathbf{R}) \\ &= \langle [u(\mathbf{R}_1) - u(\mathbf{R}_1 + \mathbf{R})]^2 \rangle \\ &\cong \langle [u'(\mathbf{R}_1) - u'(\mathbf{R}_1 + \mathbf{R})]^2 \rangle, \end{aligned} \tag{4}$$

where u' denotes the fluctuating part of the field and the brackets $\langle\rangle$ denote an ensemble average [6]. The random field $u(\mathbf{R})$ is defined statistically homogeneous when its moments are invariant under a spatial translation; in which, its mean value $\langle u(\mathbf{R})\rangle$ is independent of the spatial position $\mathbf{R}$ and the structure function depends only on the spatial vector separation $\mathbf{R} = \mathbf{R}_2 - \mathbf{R}_1$.

The velocity, temperature, and density fields are coupled to each other in the fluid flows and it is reasonable that for an optical wave propagating through a random medium, the AA fluctuations field at the end of the propagation path also to be coupled with the mentioned atmospheric fields. In this regard, we introduce the structure function for the data of the AA fluctuations measured on the entrance pupil of the second telescope. Then, we will try to investigate its inhomogeneity by the following way. We know that from the displacement of the moiré fringes in a moiré deflectometer only one component of the AA fluctuations is measurable. Therefore, for each component of the AA fluctuations obtained from the corresponding moiré deflectometer, a structure function of AA component fluctuations can be defined. We choose a coordinate system so that in the first moiré deflectometer the grating rulings are in the x-direction (parallel to the Earth surface) and those in the second moiré deflectometer are in the y-direction (perpendicular to the Earth surface). Here, the z-direction is in the propagation direction and is parallel to the Earth surface, too.

In the investigation of the inhomogeneity of the structure function of the AA fluctuations field, we need to show that its moments are not invariant under a spatial translation. For this purpose, we evaluate the structure function of the x component of the AA fluctuations field from the displacements data of the two moiré fringes with different altitudes shown by the blue traces in Fig. 2(b) left column. We know that, from the displacements of the horizontal moiré fringes shown in Fig. 2(c), the fluctuations of AA component in the x-direction are obtained. Two typical moiré fringes at two almost fixed altitudes of y_1 and $y_2 = y_1 + \Delta y$, having a separation of Δy are marked by the blue traces. From the measured fluctuations of the AA component in the x-direction over these traces, the structure functions of the x component of the AA fluctuations can be expressed in the form

$$\begin{aligned} D^{y_1}_{\alpha_x}(x_1, x_2) &\equiv D^{y_1}_{\alpha_x}(x) \\ &= \langle [\alpha_x(x_1, y_1) - \alpha_x(x_1 + x, y_1)]^2 \rangle, \end{aligned} \tag{5}$$

and

$$\begin{aligned} D^{y_1+\Delta y}_{\alpha_x}(x_1, x_2) &\equiv D^{y_2}_{\alpha_x}(x) \\ &= \langle [\alpha_x(x_1, y_2) - \alpha_x(x_1 + x, y_2)]^2 \rangle, \end{aligned} \tag{6}$$

for the upper fringe and the lower fringe, respectively.

Similarly, we evaluate that the structure function of the y component of the AA fluctuations field over two typical moiré fringes at different latitudes is shown by the red traces in Fig. 2 (b) right column. From the displacements of the vertical moiré

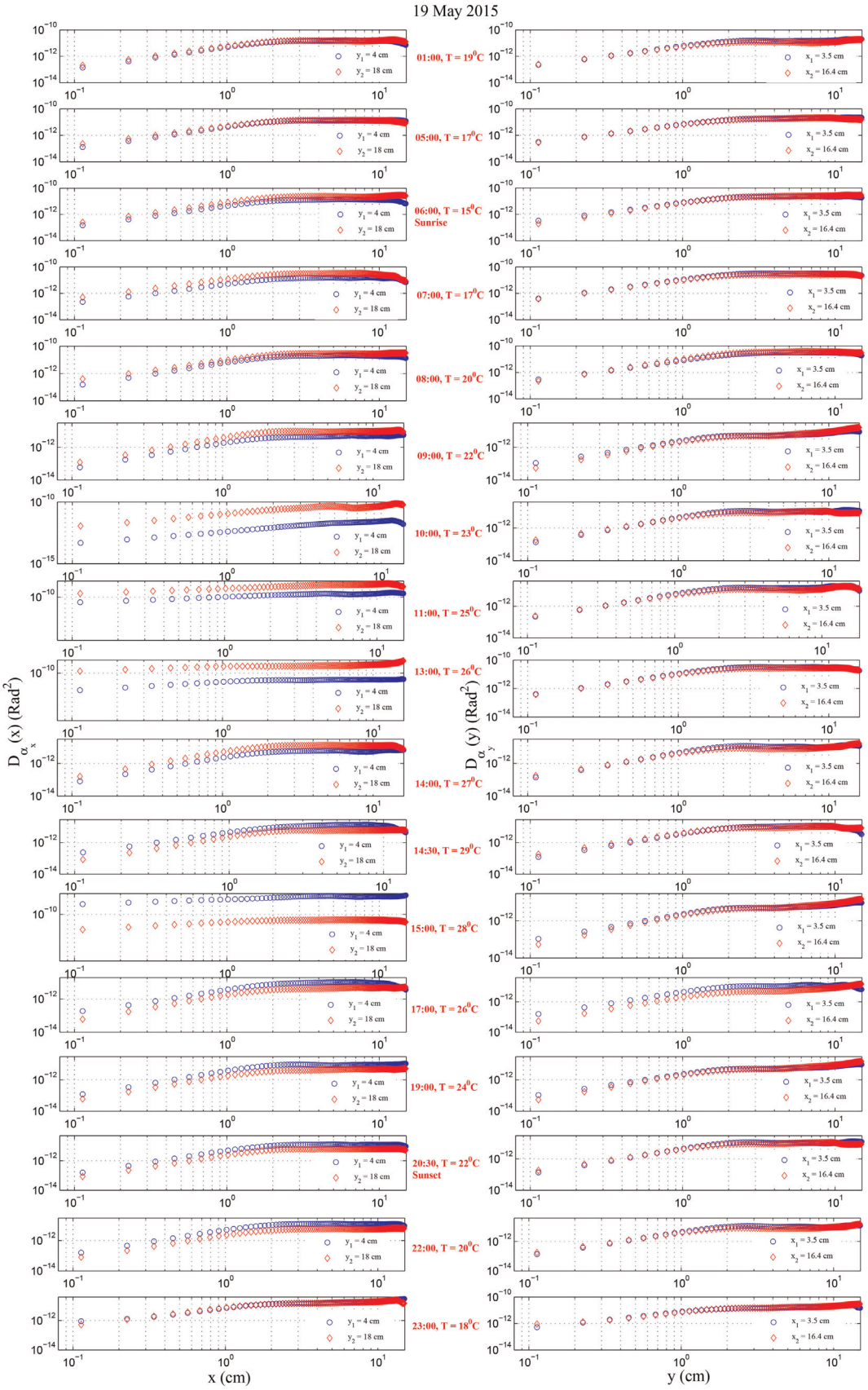

Fig. 3. Calculated plots of the structure functions of the *x* and *y* components of the AA fluctuations over the denoted traces of the moiré fringes of Fig. 2(c) for the data collected at different day and night times on May 19, 2015. This day was a sunny day. Recording time and local temperate at the recoding time are shown on the plots.

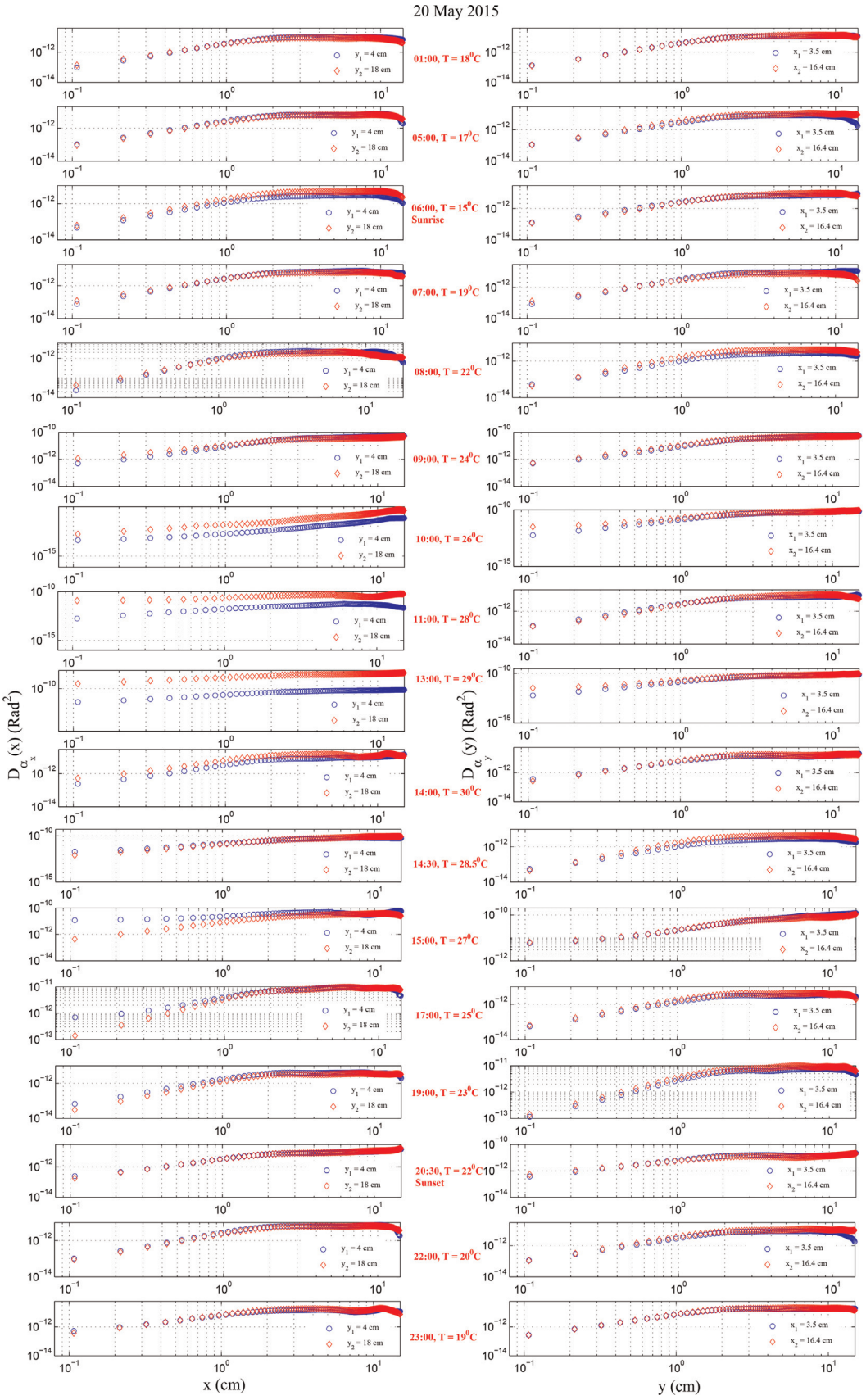

Fig. 4. Calculated plots of the structure functions of the *x* and *y* components of the AA fluctuations over the denoted traces of the moiré fringes of Fig. 2(c) for the data collected at different day and night times on May 20, 2015. This day was a sunny day.

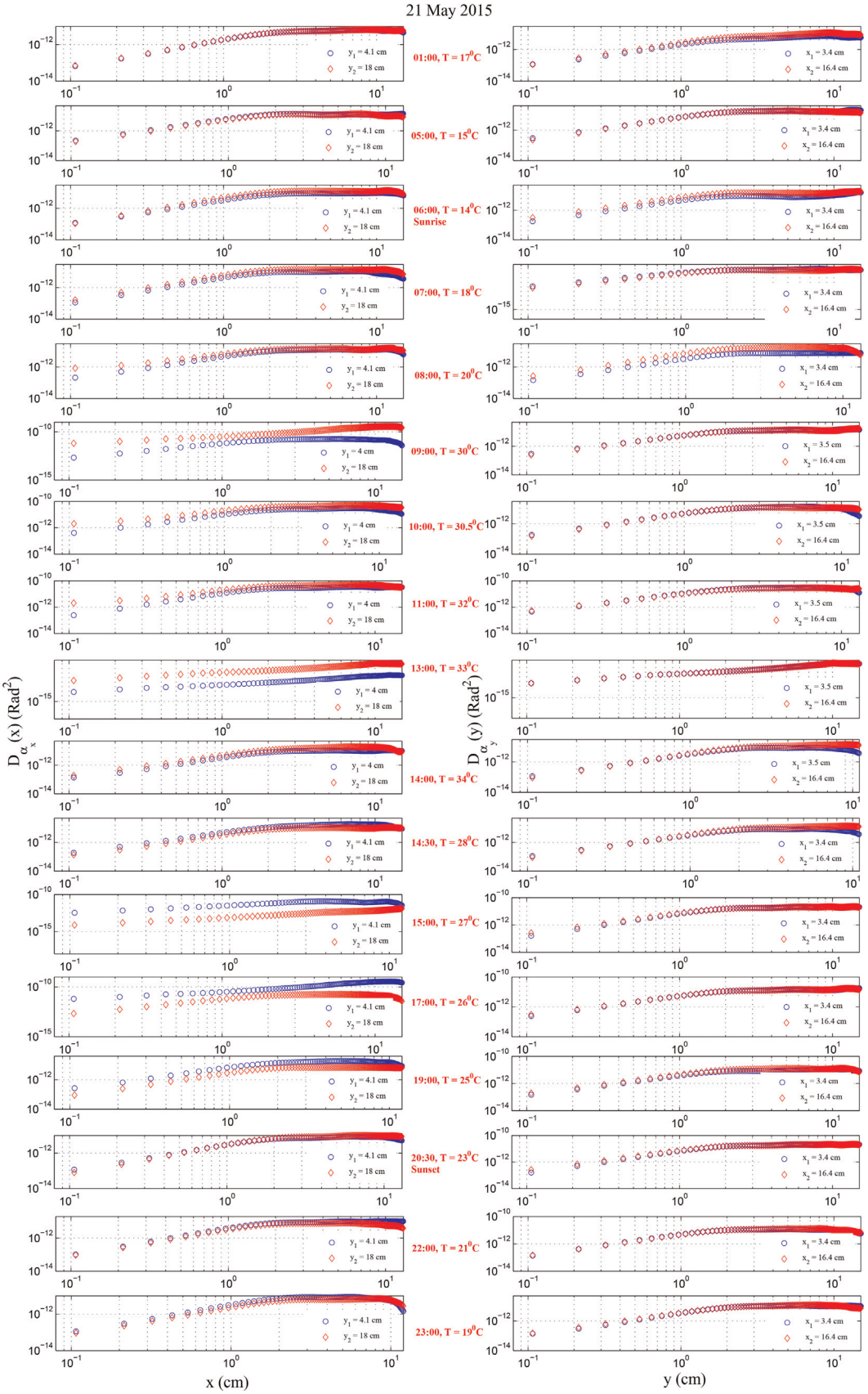

Fig. 5. Calculated plots of the structure functions of the *x* and *y* components of the AA fluctuations over the denoted traces of the moiré fringes of Fig. 2(c) for the data collected at different day and night times on May 21, 2015. This day was almost windy day.

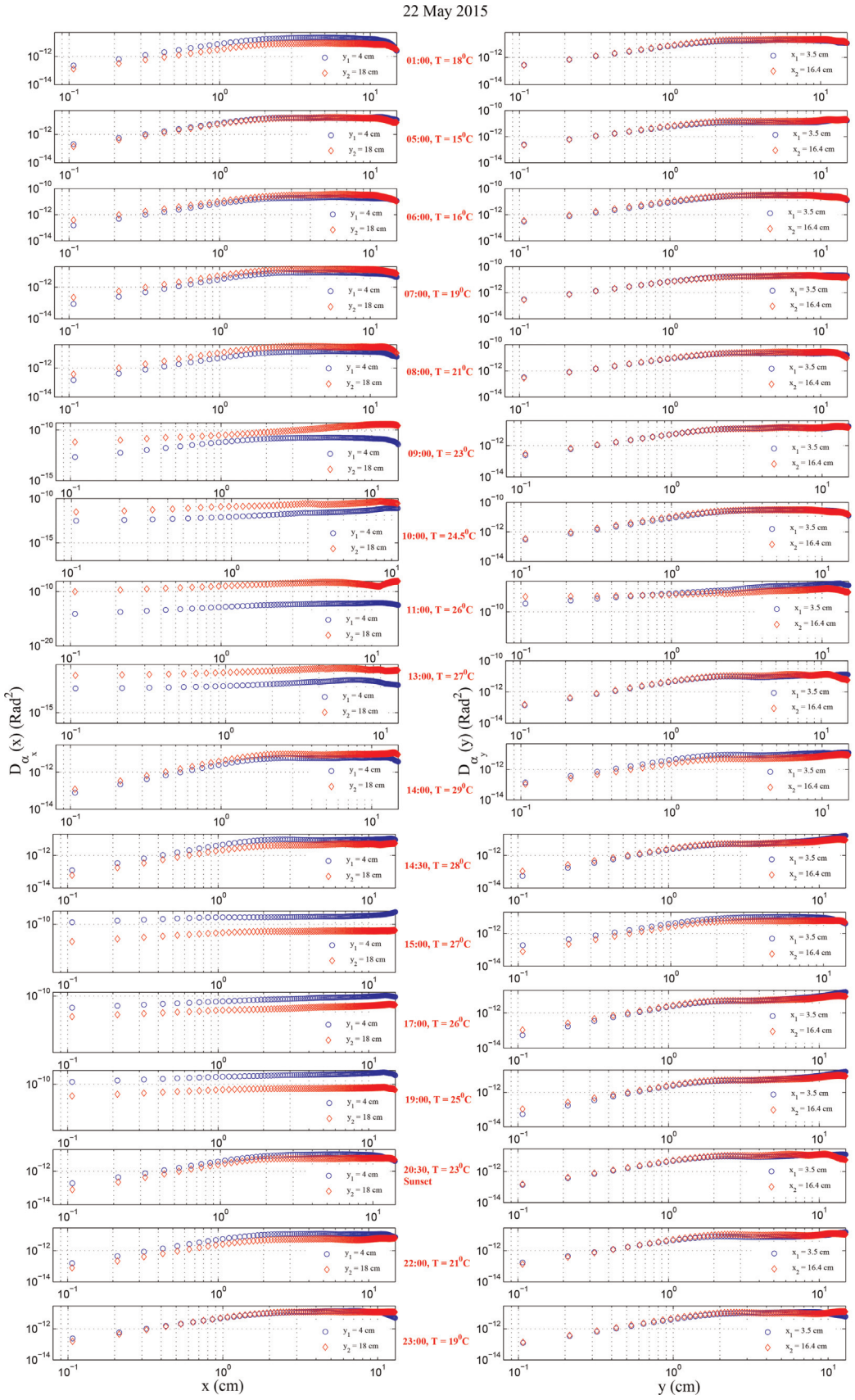

Fig. 6. Calculated plots of the structure functions of the *x* and *y* components of the AA fluctuations over the denoted traces of the moiré fringes of Fig. 2(c) for the data collected at different day and night times on June 25, 2015. This day was a sunny day.

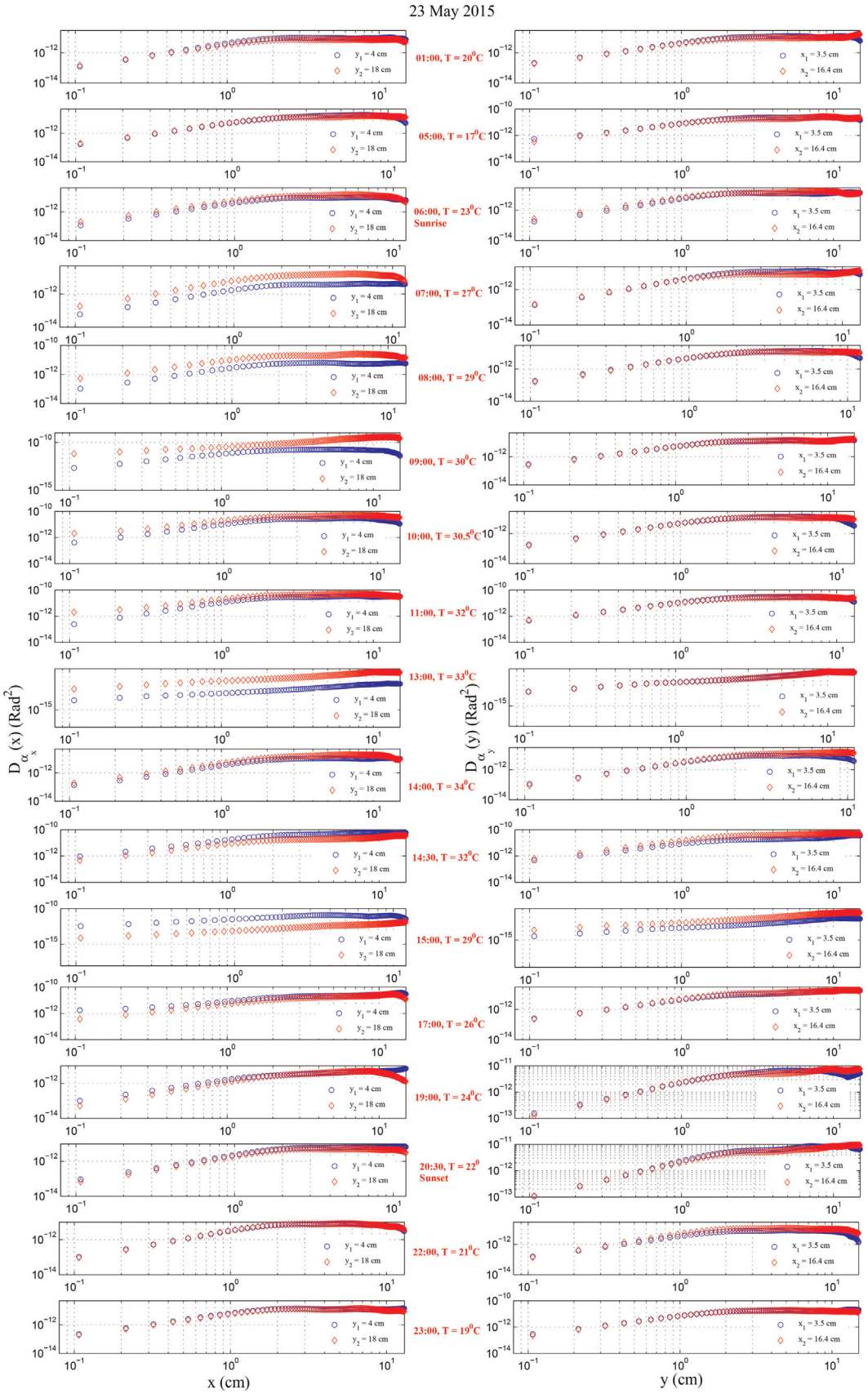

Fig. 7. Calculated plots of the structure functions of the *x* and *y* components of the AA fluctuations over the denoted traces of the moiré fringes of Fig. 2(c) for the data collected at different day and night times on May 23, 2015. This day was a sunny day.

fringes shown in Fig. 2(c), the fluctuations of the AA component in the y-direction are obtained. Two typical moiré fringes at two mean latitudes of x_1 and $x_2 = x_1 + \Delta x$ having a separation of Δx are marked by the red traces. From the measured fluctuations of the AA component in the y-direction, the structure functions of the fluctuations of the AA component in the y-direction at the latitudes x_1 and $x_2 = x_1 + \Delta x$ can be expressed in the form

$$D_{\alpha y}^{x_1}(y_1, y_2) \equiv D_{\alpha y}^{x_1}(y) = \langle [\alpha_y(x_1, y_1) - \alpha_y(x_1, y_1 + y)]^2 \rangle, \quad (7)$$

and

$$D_{\alpha y}^{x_1+\Delta x}(y_1, y_2) \equiv D_{\alpha y}^{x_2}(y) \quad (8)$$

$$= \langle [\alpha_y(x_2, y_1) - \alpha_y(x_2, y_1 + y)]^2 \rangle, \quad (9)$$

for the left fringe and right fringe, respectively.

4. Experimental work

In the experiment, the second harmonic of a CW diode pumped Nd-YAG laser beam enters a telescope (a 14 in Celestron Schmidt–Cassegrain telescope) by virtue of a focusing lens and is expanded and recollimated by it before passing horizontally through the turbulent ground level atmosphere and enters the second telescope's (The Meade 8 in Schmidt–Cassegrain model) aperture. The source, the telescopes, and the experimental set-up are installed at the height of 110 cm, over an asphalted area. The telescopes are 76 m apart. The lenses *FL* and *CL* of focal lengths 1.5 cm and 13.5 cm are used for focusing and collimating of the beam, respectively. The focusing lens is an aspheric lens. In the experiment G2 and G4 are installed at a distance of 75 mm from G1 and G3, respectively. All the gratings are identical and have a spatial period of 1/10 mm. Moiré patterns are formed on a plane where the G2 and G4 and a diffuser, D, are installed. Using a projection lens, PL, both of the moiré patterns are projected on a CCD (The Imaging Source, model DMK 21AU04, USB CCD Monochrome Camera) which is connected to a computer. After alignment of the set-up, the beam intensity was reduced by a neutral density filter to a level below the saturation level of the CCD. The moiré patterns were recorded by sampling rate of 60 frames/s and the exposure time of the frames was 1/900 s.

Several sets of the experimental data were recorded and digitized. In this report, we refer to the typical series of the measurements performed on May 19–24, 2015. Each set of data was collected in 50 s and contained 3000 frames. A typical recorded frame is shown in Fig. 2(a). To get more clearer fringes the high frequency illumination of the pattern is removed by fast Fourier transform using MATLAB software, Fig. 2(b). The traces of two bright moiré fringes were derived on the vertical and horizontal moiré patterns (see Fig. 2(b)). In the image of Fig. 2(b), the separation of the two horizontal moiré fringes marked by the blue color, Δy, and the separation of the two vertical moiré fringes marked by the red color, Δx, are equal to 14.1 cm and 13.9 cm in the real space on the second telescope's aperture plane, respectively. In this work, we have determined the traces within pixel/10 accuracy [8].

The displacements of the traces were calculated with respect to their mean positions. From the magnitude of the displacements of the vertical traces in the x-direction and the displacements of the horizontal traces in the y-direction and using Eq. (3) the fluctuations of the AA components in the corresponding directions were obtained.

Calculated plots of the structure functions of the x and y components of the AA fluctuations over the denoted traces of the

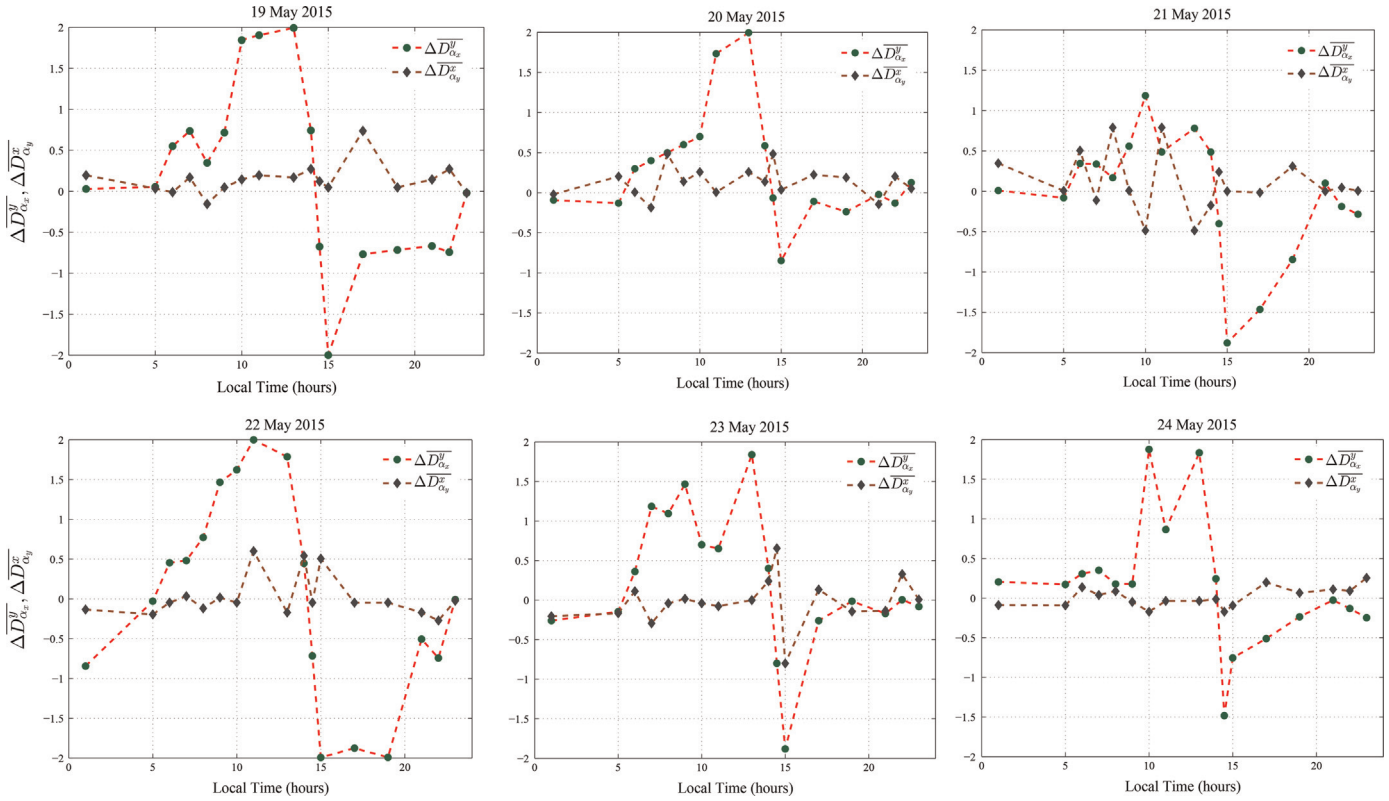

Fig. 8. The vertical and horizontal inhomogeneity coefficients, $\Delta\overline{D_{\alpha x}^{y}}$ and $\Delta\overline{D_{\alpha y}^{x}}$ are plotted as functions of the day and night times for six days of May 20–24, 2015. The observed inhomogeneity on the structure function of the x component of the AA fluctuations corresponds to the vertical separation of $\Delta y = 14.1$ cm. All of days were sunny except May 21, 2015 that was almost windy day.

moiré fringes of Fig. 2(c) using Eqs. (5)–(8) for the data collected at different day and night times in May 19, 2015 are shown in Fig. 3. Similar plots are shown in Figs. 4–8 for the structure functions calculated for the data collected on May 20–23, 2015. All of days were sunny excluding May 21, 2015 that was a windy day. On all of the plots, the recoding time and local temperature are presented.

The presented experimental results in Figs. 4–8 show that the difference between the structure functions of the horizontal component of the AA fluctuations calculated at the two different altitudes over the two horizontal moiré fringes is changed as a function of time and its value meaningfully correlated to the mean value of the temperature of the Earth's surface. For the difference between the structure functions of the vertical component of the AA fluctuations calculated at the two different latitudes over the two vertical moiré fringes there is no any interpretative correlation. In addition, for the data recorded on the windy day, May 21, 2015, the observed behavior almost disappeared. For better illustration of the above-mentioned behavior of the inhomogeneity, let us define an inhomogeneity coefficient as a ratio of the difference between the mean values of the structure functions of the AA fluctuations calculated at the two different altitudes over the two horizontal moiré fringes to the mean value of their mean values by

$$\Delta\overline{D^{y}_{\alpha x}} = \frac{\overline{D^{y_1}_{\alpha x}} - \overline{D^{y_2}_{\alpha x}}}{(\overline{D^{y_1}_{\alpha x}} + \overline{D^{y_2}_{\alpha x}})/2}, \tag{10}$$

where $\overline{D^{y_1}_{\alpha x}} = (1/N)\sum_{i=1}^{N} D^{y_1}_{\alpha x}(x_i)$ and N denotes the total number of the pixels covering the length of the corresponding moiré fringe's trace. Similarly, the ratio of the difference between the mean values of the structure functions of the AA fluctuations calculated at the two different latitudes over the two vertical moiré fringes to the mean value of their mean values can be defined by

$$\Delta\overline{D^{x}_{\alpha y}} = \frac{\overline{D^{x_1}_{\alpha y}} - \overline{D^{x_2}_{\alpha y}}}{(\overline{D^{x_1}_{\alpha y}} + \overline{D^{x_2}_{\alpha y}})/2}, \tag{11}$$

where $\overline{D^{x_1}_{\alpha y}} = (1/N)\sum_{i=1}^{N} D^{x_1}_{\alpha y}(y_i)$ and here also N denotes the total number of the pixels covering the length of the corresponding moiré fringe's trace.

All of details are shown in Fig. 8, where $\Delta\overline{D^{y}_{\alpha x}}$ and $\Delta\overline{D^{x}_{\alpha y}}$ are plotted as functions of day and night times for six days of May 20–24, 2015.

5. Conclusion

In this work, for the first time, we introduced the use of a pair of telescopes standing face to face in conjunction with the use of a pair of moiré deflectometers for observing the inhomogeneity in the statistical properties of the turbulent ground level atmosphere. The behavior of the observed inhomogeneity in the atmospheric turbulence at the day and night times was investigated. We find a significant inhomogeneity for the structure function of horizontal component of the AA fluctuations. At the two altitudes the mentioned structure functions were measured and their difference values were calculated at the day and night times. This calculation was done for the data recorded during six days from May 19 to 24, 2015. We observed a good correlation between the inhomogeneity of the structure function and changes of the Earth surface layer's temperature. In addition, for the data recorded on the windy days the observed behavior almost disappeared. It seems that in the presence of wind, the existence temperature gradient near the Earth's surface is removed by the wind and as a result the turbulence goes to the homogeneous state. Finally, the use of a pair of telescopes face to face, in conjunction with the use of a pair of moiré deflectometers, can be used for the investigation of other issues concerning the atmospheres statistical behavior such as the anisotropy and power laws different from the Kolmogorov law.

References

[1] I. Toselli, Introducing the concept of anisotropy at different scales for modeling optical turbulence, J. Opt. Soc. Am. A 31 (2014) 1868–1875.
[2] D. Dayton, B. Pierson, B. Spielbusch, J. Gonglewski, Atmospheric structure function measurements with a Shack–Hartmann wave-front sensor, Opt. Lett. 17 (1992) 1737–1739.
[3] T.W. Nicholls, G.D. Boreman, J.C. Dainty, Use of a Shack–Hartmann wave-front sensor to measure deviations from a Kolmogorov phase spectrum, Opt. Lett. 20 (1995) 2460–2462.
[4] V.P. Lukin, Investigation of the anisotropy of the atmospheric turbulence spectrum in the low frequency range, Proc. SPIE 2471 (1995) 347–354.
[5] E.M. Razi, S. Rasouli, Measuring significant inhomogeneity and anisotropy in indoor convective air turbulence in the presence of 2D temperature gradient, J. Opt. 16 (2014) 045705.
[6] L.C. Andrews, R.L. Phillips, Laser Beam Propagation though Random Media, SPIE Press, USA, 2005.
[7] S. Rasouli, Use of a moiré deflectometer on a telescope for atmospheric turbulence measurements, Opt. Lett. 35 (2010) 1470.
[8] M. Dashti, S. Rasouli, Measurement and statistical analysis of the wavefront distortions induced by atmospheric turbulence using two-channel moiré deflectometry, J. Opt. 14 (2012) 095704.
[9] S. Rasouli, E. Mohammady Razi, J.J. Niemela, Investigation of the anisotropy and scaling of the phase structure function in convective air turbulence (2015), submitted for publication.
[10] S. Rasouli, M.T. Tavassoly, Application of moiré technique to the measurement of the atmospheric turbulence parameters related to the angle of arrival fluctuations, Opt. Lett. 31 (2006) 3276–3278.
[11] S. Rasouli, M. Dashti, A.N. Ramaprakash, An adjustable, high sensitivity, wide dynamic range two channel wave-front sensor based on moiré deflectometry, Opt. Express 18 (2010) 23906.
[12] M. Sarazin, F. Roddier, The ESO differential image motion monitor, Astron. Astrophys. 227 (1990) 294–300.